Synthesis, Molecular Structure, and Physical Properties of [tetrakis((methylthio)methyl)borate]$_2$M (M = Fe, Co, Ni)

Carl Ohrenberg,[†] Pinghua Ge,[†] Peter Schebler,[†] Charles G. Riordan,*[,†] Glenn P. A. Yap,[‡] and Arnold L. Rheingold[‡]

Departments of Chemistry, Kansas State University, Manhattan, Kansas 66506, and University of Delaware, Newark, Delaware 19716

Received August 29, 1995[⊗]

The synthesis and characterization of a series of [RTt]$_2$M (RTt$^-$ = tetrakis((methylthio)methyl)borate; M = Fe, Co, Ni) complexes are reported. Isostructural derivatives of the newly synthesized phenyltris((methylthio)methyl)-borate (PhTt$^-$) also have been prepared and characterized. In each case, the ligand provides tridentate, face-capping coordination to the divalent metal ion. The Fe(II) complexes exhibit spin-crossover behavior both in solution and in the solid state. For [PhTt]$_2$Fe, the temperature dependence of μ_{eff} has been mapped between 5 K (1.3 μ_B) and 400 K (3.2 μ_B). The low-spin Co(II) derivatives exhibit characteristic axial EPR spectra; for [PhTt]$_2$Co, $g_\perp = 2.185$, $g_\parallel = 2.035$, $A_\perp = 55$ G, and $A_\parallel = 42$ G. Using O_h Fe(II) and Co(II) derivatives as benchmarks, the ligand field strength imparted by these anions is significant and falls just below that of the neutral macrocycle 1,4,7-trithiacyclononane (ttcn). All complexes have been characterized by X-ray diffraction. X-ray data: [PhTt]$_2$Fe·0.6Et$_2$O, monoclinic space group $C2/c$, with $a = 22.293(4)$ Å, $b = 12.842(8)$ Å, $c = 15.326(2)$ Å, $\beta = 130.28(6)°$, $V = 3347.4(5)$ Å^3, and $Z = 4$; [RTt]$_2$Co, triclinic space group $P\bar{1}$, with $a = 8.396(6)$ Å, $b = 8.850(2)$ Å, $c = 9.124(4)$ Å, $\alpha = 107.43(2)°$, $\beta = 92.20(4)°$, $\gamma = 94.50(4)°$, $V = 643.0(3)$ Å^3, and $Z = 1$; [PhTt]$_2$Co, monoclinic space group $P2_1/c$, with $a = 8.821(1)$ Å, $b = 14.127(8)$ Å, $c = 12.055(3)$ Å, $\beta = 103.93(2)°$, $V = 1458.0(5)$ Å^3, and $Z = 2$; [RTt]$_2$Ni, triclinic space group $P\bar{1}$, with $a = 8.607(3)$ Å, $b = 8.876(3)$ Å, $c = 9.173(3)$ Å, $\alpha = 107.44(2)°$, $\beta = 92.92(2)°$, $\gamma = 93.38(2)°$, $V = 665.70(3)$ Å^3, and $Z = 1$; [PhTt]$_2$Ni: triclinic space group $P\bar{1}$, with $a = 8.627(7)$ Å, $b = 8.862(4)$ Å, $c = 10.559(6)$ Å, $\alpha = 75.08(4)°$, $\beta = 76.64(5)°$, $\gamma = 72.71(5)°$, $V = 734.3(8)$ Å^3, and $Z = 1$.

Introduction

The coordination chemistry of three ligand types (Chart 1A−C) which present a face-capping, tridentate donor set to metal ions has been extensively developed over the last several decades.[1] The ligand field properties of these systems have permitted them to find utility in bioinorganic[2] and organometallic[3] chemistry and in coordination compounds which possess new and unusual magnetic properties.[4] While superficially similar in providing a *fac*-X$_3$ donor set, each imparts significantly different electronic and structural properties to their metal complexes resulting in distinctive reactivity patterns. Even within the same ligand set, substitution (on the pyrazole ring or N-alkylation in the case of tacn) results in considerable changes at the metal center which are manifest in rich and diverse reactivities. For example, while the unsubstituted hydrotris(pyrazolyl)borate forms six-coordinate, bis complexes with divalent metal ions, Bu^t substitution at the 3-position of the pyrazole ring blocks this reaction and allows access to pseudo-T_d geometries, e.g. [HB(3-Bu^{t}pz)$_3$]MX.[5] Unfortunately,

Chart 1

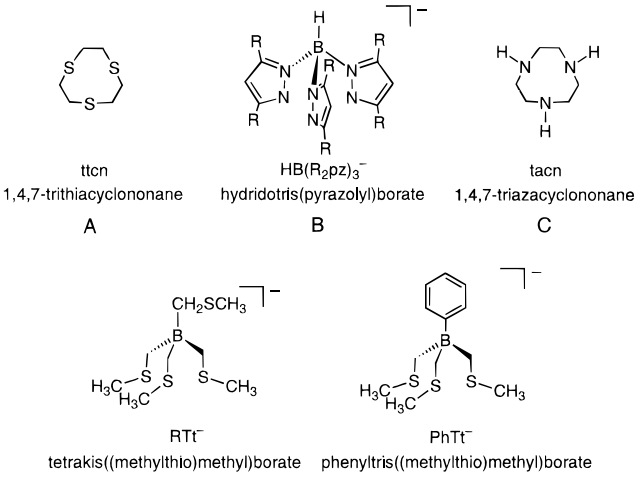

similar modifications are not possible for ttcn, as the S donors are already saturated. To circumvent this limitation for a S$_3$ donor set and to afford a S$_3^-$ donor, we recently prepared a series of poly((methylthio)methyl)borates and established their donor aptitudes via the synthesis of a range of metal complexes.[6] Herein we extend the coordination chemistry of this ligand set with the report of the synthesis, spectroscopic properties, and molecular structures of Fe(II), Co(II), and Ni(II) derivatives of tetrakis((methylthio)methyl)borate, [RTt]$_2$M, and phenyltris-((methylthio)methyl)borate, [PhTt]$_2$M. The molecular structure of [RTt]$_2$Fe has been reported.[6] The donor ability of the ligands

* To whom correspondence should be addressed. E-mail: Riordan@ksu.ksu.edu.
[†] Kansas State University.
[‡] University of Delaware.
[⊗] Abstract published in *Advance ACS Abstracts,* January 1, 1996.

(1) (a) Trofimenko, S. *Chem. Rev.* **1993**, *93*, 943−980. (b) Cooper, S. P. *Acc. Chem. Res.* **1988**, *21*, 141−146. (c) Chaudhuri, P.; Wieghardt, K. *Prog. Inorg. Chem.* **1987**, *35*, 329.
(2) For example: Mani, F. *Coord. Chem. Rev.* **1992**, *120*, 325−359.
(3) For one recent example, see: Pérez, P. J.; White, P. S.; Brookhart, M.; Templeton, J. L. *Inorg. Chem.* **1994**, *33*, 6050−6056.
(4) (a) Hotzelmann, R.; Wieghardt, K. *Inorg. Chem.* **1993**, *32*, 114−116. (b) Delfs, C.; Gatteschi, D.; Pardi, L.; Sessoli, R.; Wieghardt, K.; Hanke, D. *Inorg. Chem.* **1993**, *32*, 3099−3103.
(5) Trofimenko, S. *Prog. Inorg. Chem.* **1986**, *34*, 115−210.
(6) Ge, P.; Haggerty, B. S.; Rheingold, A. L.; Riordan, C. G. *J. Am. Chem. Soc.* **1994**, *116*, 8406−8407.

0020-1669/96/1335-0749$12.00/0

and the structural chemistry of their resulting metal complexes are compared to those of tacn, $HB(pz)_3^-$, and ttcn.

Experimental Section

Materials and Methods. All reagents were distilled under N_2 and dried as indicated. THF, Et_2O, and benzene were freshly distilled over Na/benzophenone. TMEDA was distilled under reduced pressure. $BF_3{\cdot}Et_2O$, $C_6H_5BCl_2$, $[Fe(H_2O)_6](BF_4)_2$, $NiCl_2{\cdot}6H_2O$, $[Co(H_2O)_6](BF_4)_2$, $CHCl_3$, and absolute EtOH were used as received. Elemental analyses were performed by Desert Analytics. Electronic spectra were recorded with a SLM-Aminco 3000 diode array spectrophotometer. NMR spectra were recorded on a 400 MHz Brüker spectrometer equipped with a Sun workstation. Cyclic voltammetry was performed on a BAS 50W system. All experiments were performed in an Ar-filled glovebox in a cell consisting of a glassy carbon working electrode (1 mm), Pt wire counter electrode, and Ag/AgCl reference electrode. Solutions contained 0.1 M electrolyte ($[Bu_4N][PF_6]$) and 10 mM sample. Potentials were referenced to internal Fc/Fc^+ (+410 mV vs Ag/AgCl). EPR spectra were recorded on a Brüker ER 200D-SRC spectrometer in frozen solutions of 50:50 toluene−CH_2Cl_2 and referenced to external DPPH.

Caution! *$(CH_3)_2S$ is a flammable liquid and presents a pungent odor. The deprotonation reaction should be vented through an aqueous solution of NaOCl.*

$[Bu_4N]RTt$. $(CH_3)_2S$ (15 mL, 200 mmol) and TMEDA (19 mL, 125 mmol) were placed in a 300 mL flask under a N_2 atmosphere which was vented through an aqueous solution of NaOCl. BuLi (40 mL, 2.5 M in hexanes) was added dropwise via syringe over 5 min.[7] As the BuLi was added, the mixture became viscous yellow. After 1 h at 25 °C, the solution was heated at 45 °C for 30 min to drive off unreacted $(CH_3)_2S$. The solution was again cooled to −78 °C, and $BF_3{\cdot}Et_2O$ (3.0 mL, 25 mmol) was added via syringe. The mixture was allowed to warm to 25 °C and was then stirred for 24 h. The reaction was terminated by addition of 150 mL of H_2O. Volatile organics were removed by rotary evaporation, the aqueous solution was filtered, and the product was precipitated by addition of aqueous $[(C_4H_9)_4N]Cl$. The flocculent white product was isolated by filtration, washed with Et_2O (2 × 30 mL), and dried under vacuum. Yield: 0.50 g (4%). $[Bu_4N]RTt$ is soluble in THF, acetone, EtOH, CH_2Cl_2, and $CHCl_3$. ^1H NMR ($CDCl_3$): δ 3.24 (m, NCH_2, 8 H), 2.05 (s, SCH_3, 12 H), 1.76 (q, $^2J_{BH}$ = 4.0 Hz, BCH_2, 8 H), 1.63 (m, CH_2, 8 H), 1.45 (m, CH_2, 8 H), 1.01 (t, CH_3, 12 H). $^{13}C\{^1H\}$ NMR ($CDCl_3$): δ 58.9 (s, NCH$_2$), 35.2 (q, $^1J_{BC}$ = 40.0 Hz, BCH$_2$), 24.0 (s, CH$_2$), 20.5 (s, SCH$_3$), 19.8 (s, CH$_2$), 13.7 (s, CH$_3$). $^{11}B\{^1H\}$ NMR ($CDCl_3$): δ −16.3 (s).

$[Bu_4N]PhTt$. This compound was prepared in a procedure analogous to that for $[Bu_4N]RTt$ with $PhBCl_2$ used in place of $BF_3{\cdot}Et_2O$. Reaction with $PhBCl_2$ required 48 h to reach completion. ^1H NMR ($CDCl_3$): δ 7.54 (d, CH, 2 H), 7.04 (t, CH, 2 H), 6.84 (t, CH, 1 H), 3.15 (m, NCH_2, 8 H), 2.03 (s, SCH_3, 9 H), 1.97 (q, $^2J_{BH}$ = 4.4 Hz, BCH_2, 6 H), 1.35 (m, CH_2, 16 H), 0.97 (t, CH_3, 12 H). $^{13}C\{^1H\}$ NMR ($CDCl_3$): δ 163.3 (q, $^1J_{BC}$ = 50.2 Hz, BC), 133.4 (s, CH), 126.1 (s, CH), 122.4 (s, CH), 58.9 (s, NCH$_2$), 35.8 (q, $^1J_{BC}$ = 41.3 Hz, BCH$_2$), 24.1 (s, CH$_2$), 20.7 (s, SCH$_3$), 19.8 (s, CH$_2$), 13.9 (s, CH$_3$). Yield: 3.7 g (44%).

$[RTt]_2Fe$ and $[PhTt]_2Fe$. $[Fe(H_2O)_6][BF_4]_2$ (100 mg, 0.30 mmol) in 20 mL of THF was added to $[Bu_4N]RTt$ (295 mg, 0.60 mmol) in 20 mL of THF, yielding an emerald green solution.[6] The solution was allowed to stir overnight before the solvent was removed under reduced pressure. The resulting green solid was washed with 10 mL of water and purified by recrystallization from $CHCl_3$−Et_2O. Yield: 98 mg (58%). ^1H NMR ($CDCl_3$, 27 °C): δ 7.73 (br, SCH_3, 9 H), 7.55 (br, BCH_2, 6 H), 1.88 (br, SCH_3, 3 H), 0.90 (br, BCH_2, 2 H). $[PhTt]_2Fe$ was prepared from $[Fe(H_2O)_6][BF_4]_2$ (200 mg, 0.59 mmol) and $[Bu_4N]PhTt$ (610 mg, 1.2 mmol) in a procedure similar to that for $[RTt]_2Fe$. After removal of the solvent under vacuum, the resulting solid was washed with acetone and recrystallized from THF−Et_2O. Yield: 150 mg (45%). ^1H NMR ($CDCl_3$, 27 °C): δ 7.13 (br, CH, 2 H), 7.12 (br, CH, 2 H), 6.99 (br, CH, 1 H), 3.97 (br, SCH_3, 9 H), 3.84 (br, BCH_2, 6 H). $[RTt]_2Fe$ and $[PhTt]_2Fe$ are soluble in chlorinated hydrocarbons and are stable to both oxygen and moisture.

$[RTt]_2Co$ and $[PhTt]_2Co$. $[Co(H_2O)_6][BF_4]_2$ (340 mg, 1.0 mmol) in 50 mL of THF was added to $[Bu_4N]RTt$ (1.00 g, 2.0 mmol) in 100 mL of THF, yielding a dark brown solution. THF was removed under vacuum. The brown solid was extracted into 200 mL of benzene, the extract was filtered, and the solvent was removed under vacuum. The product was recrystallized from THF−Et_2O. Microcrystalline, brown $[RTt]_2Co$ was collected by vacuum filtration and dried under Ar. Yield: 190 mg (34%). $[PhTt]_2Co$ was prepared from $[Co(H_2O)_6][BF_4]_2$ (328 mg, 0.96 mmol) and $[Bu_4N]PhTt$ (1.00 g, 1.9 mmol) in a procedure identical to that used to prepare $[RTt]_2Co$. Yield: 265 mg (46%). Solid samples of $[RTt]_2Co$ and $[PhTt]_2Co$ decompose upon prolonged exposure (14 days) to oxygen.

$[RTt]_2Ni$ and $[PhTt]_2Ni$. $NiCl_2{\cdot}6H_2O$ (200 mg, 0.88 mmol) was added to $[Bu_4N]PhTt$ (840 mg, 1.7 mmol) in 20 mL of THF resulting in a blue-green solution. The reaction mixture was allowed to stir overnight, yielding a blue-green solid, which was collected by vacuum filtration. The solid was washed with water and recrystallized from $CHCl_3$−Et_2O. Yield: 160 mg (33%). $[PhTt]_2Ni$ was prepared by adding $[Bu_4N]PhTt$ (500 mg, 0.97 mmol) in 25 mL of EtOH to $NiCl_2{\cdot}6H_2O$ (100 mg, 0..44 mmol) in 100 mL of EtOH resulting in the immediate formation of a blue-green solid, which was collected by vacuum filtration. The precipitate was then purified in the same manner as $[RTt]_2Ni$. Yields: 220 mg (83%). Both $[RTt]_2Ni$ and $[PhTt]_2Ni$ are stable to air and moisture.

	anal.	
	% C (calc)	% H (calc)
$[RTt]_2Fe$ ($C_{16}H_{40}B_2FeS_8$)	33.89 (33.93)	7.16 (7.12)
$[PhTt]_2Fe$ ($C_{24}H_{40}B_2FeS_6$)	48.22 (48.17)	6.70 (6.74)
$[RTt]_2Co$ ($C_{16}H_{40}B_2CoS_8$)	33.67 (33.74)	6.94 (7.08)
$[PhTt]_2Co$ ($C_{24}H_{40}B_2CoS_6$)	47.78 (47.92)	6.65 (6.70)
$[RTt]_2Ni$ ($C_{16}H_{40}B_2NiS_8$)	33.96 (33.76)	7.25 (7.08)
$[PhTt]_2Ni$ ($C_{24}H_{40}B_2NiS_6$)	47.91 (47.94)	6.47 (6.71)

Crystallographic Structural Determinations. Crystallographic data for the structures are collected in Table 1 and in the Supporting Information. Specimens were mounted with epoxy cement on glass fibers. The unit-cell parameters were obtained by the least-squares refinement of the angular settings of 24 reflections ($20° \leq 2\theta \leq 25°$).

The systematic absences were consistent with $P2_1/c$, uniquely for $[PhTt]_2Co$, and with Cc or $C2/c$ for $[PhTt]_2Fe{\cdot}0.6Et_2O$. No evidence of symmetry higher than triclinic was observed in either the photographic or the diffraction data for $[RTt]_2Co$, $[RTt]_2Ni$, and $[PhTt]_2Ni$. *E*-statistics suggested the centrosymmetric space group options for $[PhTt]_2Fe{\cdot}0.6Et_2O$, $[RTt]_2Co$, and $[PhTt]_2Ni$. The space group choices were subsequently verified by chemically reasonable results of refinement. The structures were solved by direct methods, completed by subsequent difference Fourier syntheses, and refined by full-matrix least-squares procedures. The molecules were located on inversion centers for $[RTt]_2Co$, $[PhTt]_2Co$, $[RTt]_2Ni$, and $[PhTt]_2Ni$. In $[RTt]_2Co$, the uncoordinated ligand arm atoms, S(4) and C(7), were located in two disordered positions with a 50:50 distribution. In $[RTt]_2Ni$, the uncoordinated ligand arm atoms, S(4) and C(4), were located in two disordered positions with a 60:40 distribution. In, $[PhTt]_2Fe{\cdot}0.6Et_2O$ the molecule was located on a 2-fold axis with the sulfur atoms disordered in two positions with a 50:50 distribution. A severely disordered Et_2O solvent molecule was also located at 60% occupancy near an inversion center. All non-hydrogen atoms were refined with anisotropic displacement coefficients, except the carbon and boron atoms in $[PhTt]_2Fe{\cdot}0.6Et_2O$, which were refined isotropically. Hydrogen atoms were treated as idealized contributions except on the disordered C(7) atom in $[RTt]_2Co$, which was ignored.

All software and sources of the scattering factors are contained in either SHELXTL (5.1) or SHELXTL PLUS (4.2) program libraries (G. Sheldrick, Siemens XRD, Madison, WI).

Results and Discussion

Ligand Syntheses. RTt^- and $PhTt^-$ may be prepared conveniently as the corresponding Bu_4N^+ salts. $(CH_3)_2S$ was readily and quantitatively deprotonated by BuLi in the presence of TMEDA.[7] The resulting carbanion, $LiCH_2SCH_3$, reacted with the appropriate boron reagent ($BF_3{\cdot}Et_2O$ for RTt^- and

(7) Peterson, D. J. *J. Org. Chem.* **1967**, *32*, 1717−1720.

Table 1. Crystallographic Data

	$[PhTt]_2Fe\cdot0.6Et_2O$	$[RTt]_2Co$	$[PhTt]_2Co$	$[RTt]_2Ni$	$[PhTt]_2Ni$
formula	$C_{26.4}H_{46}B_2O_{0.6}FeS_6$	$C_{16}H_{40}B_2CoS_8$	$C_{24}H_{40}B_2CoS_6$	$C_{16}H_{40}B_2NiS_8$	$C_{24}H_{40}B_2NiS_6$
fw	642.9	569.5	601.5	569.3	601.2
color, habit	green, block	brown, block	black, block	teal, block	blue, block
crystal size, mm	0.4 × 0.4 × 0.4	0.2 × 0.3 × 0.3	0.3 × 0.3 × 0.4	0.4 × 0.5 × 0.5	0.3 × 0.4 × 0.4
crystal syst	monoclinic	triclinic	monoclinic	triclinic	triclinic
space group	$C2/c$[a]	$P\bar{1}$	$P2_1/c$	$P\bar{1}$	$P\bar{1}$
a, Å	22.293(4)	8.396(6)	8.821(1)	8.607(3)	8.627(7)
b, Å	12.842(8)	8.850(2)	14.127(3)	8.876(3)	8.862(4)
c, Å	15.326(2)	9.124(4)	12.055(3)	9.173(3)	10.559(6)
α, deg		107.43(2)		107.44(2)	75.08(4)
β, deg	130.28(6)	92.20(4)	103.93(2)	92.92(2)	76.64(5)
γ, deg		94.50(4)		93.38(2)	72.71(5)
V, Å^3	3347.4(5)	643.0(3)	1458.0(5)	665.70(3)	734.3(8)
Z	4	1	2	1	1
T, K	226	224	298	296	296
λ, Å (Mo Kα)	0.710 73	0.710 73	0.710 73	0.710 73	0.710 73
2θ range, deg	4.0−45.0	4.0−60.0	4.0−45.0	4.0−46.0	4.0−65.0
ρ(calc), g cm^{-3}	1.276	1.449	1.370	1.420	1.360
μ(Mo Kα), cm^{-1}	8.40	13.00	10.31	13.59	11.00
no. of obsd rflcns for $F > n\sigma(F)$	1613 ($n = 4$)	3200 ($n = 5$)	1393 ($n = 4$)	3936 ($n = 5$)	3284 ($n = 4$)
$R(F)$, $R_w(F)$	0.076,[b] 0.11	0.038,[b] 0.043	0.039,[b] 0.049	0.031,[b] 0.049	0.034,[c] 0.075[d]

[a] Equivalent I-centered cell ($a = 15.326(2)$, $b = 12.842(8)$, $c = 17.032(3)$ Å; $\beta = 93.07(5)°$) was used for data collection. [b] Quantity minimized $= \sum w\Delta^2$; $R = \sum\Delta/(F_o)$; $R_w = \sum[\Delta w^{1/2}]/[F_o w^{1/2}]$; $\Delta = |F_o - F_c|$. [c] Quantity minimized $= \sum[w(F_o^2 - F_c^2)^2]/\sum[(wF_o^2)^2]^{1/2}$; $R = \sum\Delta/(F_o)$; $R_w = \sum[\Delta w^{1/2}]/[F_o w^{1/2}]$; $\Delta = |F_o - F_c|$. [d] $R = wF^2$.

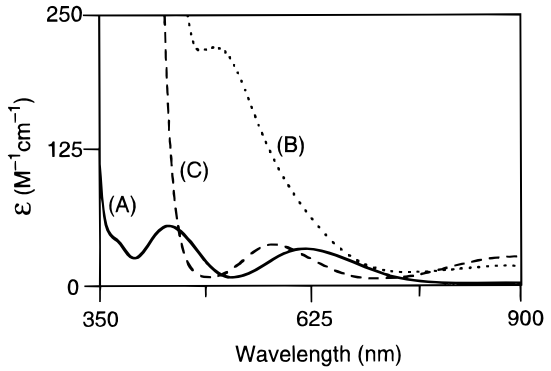

Figure 1. Electronic spectra ($CHCl_3$) of (A) $[PhTt]_2Fe$, (B) $[PhTt]_2Co$, and (C) $[PhTt]_2Ni$ at 25 °C.

$C_6H_5BCl_2$ for $PhTt^-$) to yield the desired product. The Bu_4N^+ salts were precipitated from aqueous solutions upon addition of [Bu$_4$N]Cl. [Bu$_4$N]RTt and [Bu$_4$N]PhTt are white solids stable to both oxygen and moisture. The salts are soluble in $CHCl_3$, CH_2Cl_2, THF, and acetone. Spectroscopic data are contained in the Experimental Section.

Preparation of Metal Complexes. The six-coordinate $[RTt]_2M$ and $[PhTt]_2M$ complexes of divalent Fe, Co, and Ni were prepared in moderate to high yields from THF or ethanolic solutions of the ligand and the respective metal salt, $M(H_2O)_6\cdot 2X$ (M = Fe, Co, X = BF_4; M = Ni, X = Cl), in the molar ratio of 2:1. The resulting metal complexes were isolated by extraction with $CHCl_3$ or C_6H_6 and purified by recrystallization from $CHCl_3-Et_2O$. Satisfactory elemental analyses have been determined for all complexes (Experimental Section), while spectroscopic data are discussed below. In all cases, the $PhTt^-$ derivatives enjoyed greater solubility than their RTt^- counterparts. While the Fe and Ni species are stable to O_2, $[RTt]_2Co$ and $[PhTt]_2Co$ readily decompose in solution (and more slowly (days) in the solid state) under O_2.

Electronic Spectra. The electronic spectra of $[PhTt]_2M$ (M = Fe, Co, Ni) are contained in Figure 1, and pertinent data are given in Table 2. $[PhTt]_2Fe$ displayed two d−d transitions consistent with low-spin Fe(II) in an octahedral ligand field. Measuring the energy difference between these two maxima and assuming $C = 4B$ yielded values for D_q of 1763 cm^{-1} and B of 420 cm^{-1}. Using L_2Fe complexes as a benchmark, the ligand field strength of $PhTt^-$ is somewhat less than those of both (D_q = 2067 cm^{-1}) and tacn (D_q = 1894 cm^{-1}).[8] The electronic spectrum of $[PhTt]_2Co$ displayed two d−d transitions and one charge transfer transition in agreement with a low-spin, d^7 configuration. The d−d bands are assigned to $^2E_g \rightarrow {}^2T_{1g}$ (890 nm) and $^2E_g \rightarrow {}^2T_{2g}$ (504 nm). $[PhTt]_2Ni$ displayed an intense charge transfer transition at 369 nm ($\epsilon = 1 \times 10^4$ M^{-1}cm^{-1}) and a single d−d transition at 578 nm. The latter is assigned to the transition $^3A_{2g} \rightarrow {}^3T_{1g}(^3F)$. The high-energy $^3A_{2g} \rightarrow {}^3T_{1g}(^3P)$ transition is hidden under the charge transfer band, while the low-energy transition $^3A_{2g} \rightarrow {}^3T_{2g}$ occurs slightly above 900 nm, outside the limit of our spectrophotometer.

Table 2. Electronic Spectral Data and Magnetic Moments for $[RTt]_2M$ and $[PhTt]_2M$ Complexes

compd	λ, nm (ϵ, M^{-1}cm^{-1})[a]	μ_{eff}, μ_B[b]
$[RTt]_2Fe$	627 (46), 441 (79)	1.8
$[PhTt]_2Fe$	627 (33), 439 (56)	1.6
$[RTt]_2Co$	490 (210) sh, 382 (6300), 338 (6500)[c]	2.4
$[PhTt]_2Co$	504 (260), 380 (7400), 337 (6800)[c]	2.2 (2.3)
$[RTt]_2Ni$	581 (41), 368 (9000)	3.1
$[PhTt]_2Ni$	578 (37), 369 (10,000)	3.0 (3.1)

[a] Measured in $CHCl_3$. [b] Measured in $CDCl_3$ at 27 °C (solid state value). [c] Measured in CH_2Cl_2.

Proton NMR Spectra. The temperature-dependent ^{1}H NMR spectrum of $[RTt]_2Fe$ in $CDCl_3$ displayed four broad, unresolved resonances at 27 °C. The two upfield lines are assigned to the methylene (0.91 ppm) and methyl (1.89 ppm) protons of the unligated thioether. The Fe-bound thioether methylene (7.50 ppm) and methyl (7.68 ppm) protons resonate at lower field and exhibit broadened lines. Upon an increase in temperature to 50 °C, the downfield methylene and methyl resonances shift further downfield (*ca.* 16 ppm) and significantly broaden ($\Delta\nu_{1/2}$ = 240 Hz) while the other thioether proton resonances virtually remain unchanged. These spectra are consistent with a static structure in which the thioether arms are not equilibrating on the NMR time scale. Similar static behavior has been observed for $[Bu_4N][[RTt]Mo(CO)_3]$.[6] While the electronic spectrum is

(8) Wieghardt, K.; Küppers, H.-J.; Weiss, J. *Inorg. Chem.* **1985**, *24*, 3067−3071.

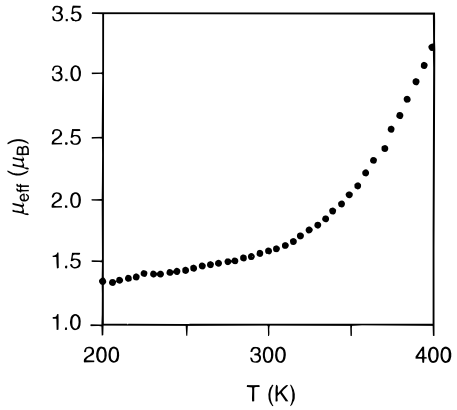

Figure 2. Plot of μ_{eff} vs T for a powdered sample of $[PhTt]_2Fe$.

in accord with a low-spin configuration, the broadness of the proton resonances, the unusual chemical shifts of the bound thioether protons, and the temperature-dependent behavior of the ^1H NMR suggest some contribution from an energetically accessible high-spin state. As detailed below, both $[RTt]_2Fe$ and $[PhTt]_2Fe$ exhibit spin-crossover behavior in the solid state, consistent with the moderately strong ligand field provided by the poly((methylthio)methyl)borate ligands.[9] Paramagnetic $[PhTt]_2Co$ and $[PhTt]_2Ni$ do not provide useful ^1H NMR spectra.

Magnetic Properties. Magnetic susceptibilities were measured both in solution by Evans' NMR method and in the solid state by the Faraday method. Effective magnetic moments are given in Table 2. In all cases, good agreement was observed between the two methods. The Co(II) complexes possessed magnetic moments of 2.2 μ_B, consistent with a low-spin, d^7 electronic configuration, $S = {}^1/_2$. This electron distribution was corroborated by electronic and EPR spectroscopies and the molecular structures as determined by X-ray diffraction. While Co(II) in a low-spin configuration is not common, hexakis(thioether) coordination does provide sufficient ligand field splitting to achieve this spin state. For example, both $(ttcn)_2Co^{2+}$ and $(18S_6)Co^{2+}$ are low-spin.[10]

$[PhTt]_2Ni$ and $[RTt]_2Ni$ have magnetic moments in $CDCl_3$ of 3.0 and 3.1 μ_B, respectively, indicative of two unpaired spins for the d^8 configuration in an O_h ligand field.

The magnetic susceptibilities of the Fe(II) complexes were found to be temperature-dependent. At 27 °C, the effective magnetic moments in $CDCl_3$ were 1.8 μ_B for $[RTt]_2Fe$ and 1.6 μ_B for $[PhTt]_2Fe$. The temperature dependence of μ_{eff} for a powdered sample of $[PhTt]_2Fe$ is shown in Figure 2. The effective magnetic moment essentially remained constant between 5 and 200 K. From 200 to 400 K, the limit of the SQUID magnetometer, the value increased from 1.3 to 3.2 μ_B. The temperature dependence is attributed to spin-crossover behavior in which an excited, high-spin electronic state ($^5T_{2g}$, $S = 2$) is accessible from the diamagnetic ground state ($^1A_{1g}$, $S = 0$).[11] Again, this behavior is in accord with the strength of the ligand field provided by $PhTt^-$.

Electrochemistry. Electrochemical data for $[Bu_4N]PhTt$ and the metal complexes in CH_2Cl_2 are contained in Table 3.

Table 3. Electrochemical Data for $[[RTt]_2M$ and $[PhTt]_2M$ Complexes

compd	E_f, V[a]	ΔE_p, mV	$I_{p,a}/I_{p,c}$	
$[Bu_4N]PhTt$	0.08			irrev
	0.79			irrev
$[RTt]_2Fe$	0.08	247		quasi-rev
$[PhTt]_2Fe$	0.09	96	1.5	quasi-rev
$[RTt]_2Co$	−0.54	96	0.97	rev
	−1.15			irrev
$[PhTt]_2Co$	−0.53	97	0.90	rev
	−1.60			irrev
$[RTt]_2Ni$	−0.30			irrev
	−1.78			irrev
$[PhTt]_2Ni$	−1.01			irrev
	−1.87			irrev

[a] vs Fc/Fc^+ in CH_2Cl_2.

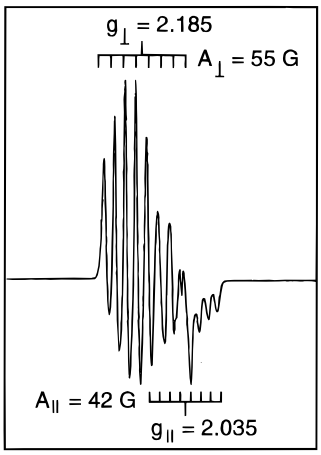

Figure 3. EPR spectrum of $[PhTt]_2Co$ in toluene−CH_2Cl_2 glass at 77 K.

Formal potentials are referenced to internal Fc/Fc^+. The uncoordinated ligand exhibited two irreversible oxidations at 0.08 and 0.79 V. The product(s) of these oxidations has (have) not been identified. $[PhTt]_2Fe$ showed an electrochemically reversible Fe(III/II) couple slightly anodic of Fc/Fc^+ but at significantly lower potential than that for $(ttcn)_2Fe^{2+}$.[8] The ease of oxidation of our complex relative to the ttcn system may be attributed to its overall electroneutrality. The Co(II) derivatives exhibited a reversible couple at −0.53 V and an irreversible reduction below −1.0 V. The former has been assigned to the Co(III/II) couple on the basis of chronoamperometry experiments, while the latter is attributed to the Co(II/I) couple. In contrast, $(ttcn)_2Co^{2+}$ exhibits two reversible one-electron reductions.[8] The inability of the present system to stabilize Co(I) may be a consequence of metal-mediated, ligand-based reduction facilitating S−C bond rupture and $CH_3^\bullet$ production. This decomposition path may be less accessible to the more rigid ttcn macrocycle. Consistent with this proposal, electrochemical reduction of $[PhTt]_2Ni$ is irreversible, while $(ttcn)_2Ni^{2+}$ is quasi-reversible. Current efforts are directed toward characterizing the products of chemical reduction of $[PhTt]_2Co$ and $[PhTt]_2Ni$.

Electron Paramagnetic Resonance of $[PhTt]_2Co$. Consistent with its low-spin configuration, $[PhTt]_2Co$ displayed an EPR spectrum at 77 K (Figure 3).[10] The axial spectrum exhibited $g_\perp = 2.185$ and $g_\parallel = 2.035$ referenced to external DPPH. Hyperfine coupling to ^{59}Co ($I = {}^7/_2$, 100% natural abundance) further split each feature into eight distinct lines ($A_\perp = 55$ G, $A_\parallel = 42$ G). Axial symmetry is in accord with the expected Jahn−Teller distortion of a d^7 metal ion in an approximately O_h field. Interestingly, the EPR spectrum of $[RTt]_2Co$ (not

(9) (a) Jesson, J. P.; Trofimenko, S.; Eaton, D. R. *J. Am. Chem. Soc.* **1967**, *89*, 3158−3164. (b) Hutchinson, B.; Daniels, L.; Henderson, E.; Neill, P.; Long, G. J.; Becker, L. W. *J. Chem. Soc., Chem. Commun.* **1979**, 1003−1004.

(10) (a) Setzer, W. N.; Ogle, C. A.; Wilson, G. S.; Glass, R. S. *Inorg. Chem.* **1983**, *22*, 266−271. (b) Hartman, J. R.; Hintsa, E. J.; Cooper, S. R. *J. Chem. Soc., Chem. Commun.* **1984**, 386−387. (c) Hartman, J. R.; Hintsa, E. J.; Cooper, S. R. *J. Am. Chem. Soc.* **1986**, *108*, 1208−1214. (d) Wilson, G. S.; Swanson, D. D.; Glass, R. S. *Inorg. Chem.* **1986**, *25*, 3827−3829.

(11) Drago, R. S. *Physical Methods for Chemists*, 2nd ed.; Saunders College Publishing: New York, 1992; p 489.

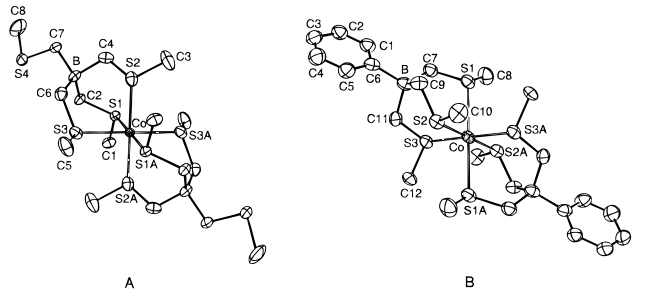

Figure 4. Thermal ellipsoid plots of (A) $[RTt]_2Co$ and (B) $[PhTt]_2Co$. Thermal ellipsoids are drawn at the 40% probability level. Hydrogen atoms are omitted for clarity.

Table 4. Selected Bond Lengths (Å) and Bond Angles (deg) for $[RTt]_2M$ and $[PhTt]_2M$ Complexes

		$[PhTt]_2Fe$	
Fe−S1	2.333(4)	S1−Fe−S2	86.3(1)
Fe−S2	2.330(4)	S2−Fe−S3	87.8(2)
Fe−S3	2.293(6)	S1−Fe−S3	86.4(2)
Fe−S1′A	2.270(4)	Fe−S1−C11	114.2(4)
Fe−S2′A	2.282(4)	Fe−S2−C10	112.6(3)
Fe−S3′A	2.288(7)	Fe−S3−C12	113.4(4)
		$[RTt]_2Co$	
Co−S1	2.262(2)	S1−Co−S3	85.0(1)
Co−S2	2.405(2)	Co−S1−C8	117.8(2)
Co−S3	2.412(2)	Co−S2−C10	114.4(2)
S1−Co−S2	88.7(1)	Co−S3−C12	111.2(2)
S2−Co−S3	87.5(1)		
		$[PhTt]_2Co$	
Co−S1	2.591(2)	S1−Co−S3	88.7(1)
Co−S2	2.294(1)	Co−S1−C1	114.5(1)
Co−S3	2.265(1)	Co−S2−C3	114.2(1)
S1−Co−S2	87.2(1)	Co−S3−C5	115.3(1)
S2−Co−S3	87.0(1)		
		$[RTt]_2Ni$	
Ni−S1	2.431(1)	S1−Ni−S3	86.7(1)
Ni−S2	2.417(1)	Ni−S1−C11	114.4(1)
Ni−S3	2.442(1)	Ni−S2−C22	114.3(1)
S1−Ni−S2	87.0(1)	Ni−S3−C33	113.6(1)
S2−Ni−S3	87.4(1)		
		$[PhTt]_2Ni$	
Ni−S1	2.438(2)	S1−Ni−S3	84.9(1)
Ni−S2	2.434(1)	Ni−S1−C11	113.4(1)
Ni−S3	2.428(2)	Ni−S2−C21	114.3(1)
S1−Ni−S2	87.1(1)	Ni−S3−C31	113.9(1)
S2−Ni−S3	87.8(1)		

shown) is essentially superimposable, despite significant differences in the molecular structures of $[RTt]_2Co$ and $[PhTt]_2Co$. As detailed below, X-ray crystallography shows that $[PhTt]_2Co$ is tetragonally elongated while $[RTt]_2Co$ is tetragonally compressed. Such differences should lead to a change in relative energies of the $g_\perp$ and $g_{||}$ features. The absence of such changes suggest that, in frozen solutions, both molecules are distorted in the same manner—tetragonal elongation.

Molecular Structures. The molecular structure of each derivative has been elucidated by X-ray diffraction. Representative examples of $[RTt]_2M$ and $[PhTt]_2M$ are contained in Figure 4. Selected metric parameters are contained in Table 4. As the $[RTt]_2M$ and $[PhTt]_2M$ series of complexes are isostructural, only their general structural features will be discussed. Each molecule contains two tridentate borate ligands resulting in a S_6-coordination environment of virtual O_h symmetry. The M atom occupies a crystallographic inversion center (except for $[PhTt]_2Fe$, in which the metal resides on a 2-fold axis) which renders *trans* thioether arms metrically equivalent. The average

Table 5. Comparative M−S Bond Lengths for $[RTt]_2M$, $[PhTt]_2M$, and $[(ttcn)_2M][X]_2$ Complexes

compd	av M−S, Å	compd	av M−S, Å
$[RTt]_2Fe$	2.303	$[(ttcn)_2Fe][PF_6]_2$[8]	2.250
$[PhTt]_2Fe$	2.303	$[(20S_6)Fe][ClO_4]_2$[12]	2.250
$[RTt]_2Co$	2.262	$[(ttcn)_2Co][BF_4]_2$[10a]	2.240
	2.412		2.367
	2.405		2.356
$[PhTt]_2Co$	2.591	$[(18S_6)Co][picrate]_2$[10b]	2.251
	2.265		2.292
	2.294		2.479
$[RTt]_2Ni$	2.430	$[(ttcn)_2Ni][BF_4]_2$[10a]	2.388
$[PhTt]_2Ni$	2.433	$[(18S_6)Ni][picrate]_2$[13]	2.387

M−S distances are significantly longer than those in the corresponding $(ttcn)_2M^{2+}$ systems reported previously, Table 5. For the Fe(II) and Ni(II) derivatives, the three distinct M−S distances are very similar within the same molecule with no systematic differences between the RTt^- and $PhTt^-$ complexes. However, for the Co(II) complexes, distinct Jahn−Teller distortions in the Co−S bond distances are observed. In $[RTt]_2Co$, there are two longer pairs of Co−S bond lengths (2.412(2) and 2.405(2) Å) and one shorter set (2.262(2) Å). These parameters are consistent with a tetragonal compression placing the unpaired electron in the $d_{x^2-y^2}$ orbital. Jahn−Teller distortions in this direction (compression) are much less common than elongations. In the case of $[PhTt]_2Co$, tetragonal elongation is observed, as evidenced by two shorter pairs of Co−S bond distances (2.265(1) and 2.294(1) Å) and one longer pair (2.591(2) Å). In the latter case, the unpaired electron resides in the d_{z^2} orbital. The forces which determine whether low-spin Co(II) distorts via elongation or contraction are unclear. However, the Jahn−Teller stabilization energy achieved by either type of distortion should be similar. Perhaps intermolecular forces in the solid state ultimately dictate the direction of distortion. EPR spectra of frozen solutions of $[RTt]_2Co$ and $[PhTt]_2Co$ support distortions in the same direction (elongation). The S−M−S bond angles about M for all complexes are within 5° of those in an idealized O_h geometry. The bound S atoms are pyramidalized with the angle between the CH_2-S-CH_3 plane and the M−S vector equal to $\angle_{av}$ 121.0°. The disposition of the thioethers is such that each SCH_3 vector is canted in the same direction, Figure 5. Presumably, this minimizes steric interactions between *cis* ligands: the opposite orientation would result in overcrowding between CH_3 groups of adjacent thioethers. Each methyl group "caps" a single *cis* sulfur (S- - -CH_3 3.29 Å) with a dihedral angle, $CH_3-S-M-S_{cis}$, of less than 2°. This orientation of the methyl groups may protect the ligand kinetically from reactions at the coordinated sulfur. While this canting renders the methylene hydrogens diastereotopic, low-temperature (−50 °C) ^{1}H NMR experiments on $[RTt]_2Fe$ were unsuccessful in completely resolving these resonances.[14] The accessibility of the Fe(II) high-spin state undoubtedly contributes to line broadening and, therefore, our inability to observe the diastereotopic resonances.

Summary. Tetrakis((methylthio)methyl)borate and phenyltris((methylthio)methyl)borate are competent ligands for first-row transition metal ions forming bis complexes of approximately O_h geometry. These derivatives display distinct

(12) Grant, G. J.; Isaac, S. M.; Setzer, W. N.; VanDerveer, D. G. *Inorg. Chem.* **1993**, *32*, 4284−4290.
(13) Hartman, J. R.; Hintsa, E. J.; Cooper, S. R. *J. Am. Chem. Soc.* **1983**, *105*, 3738−3739.
(14) The resonance for the CH_2 protons of the Fe-bound thioether broadens into the baseline at −55 °C in $CDCl_3$. However, solubility difficulties have prevented accessing a lower temperature where the two resonances for the diastereotopic protons are expected to emerge.

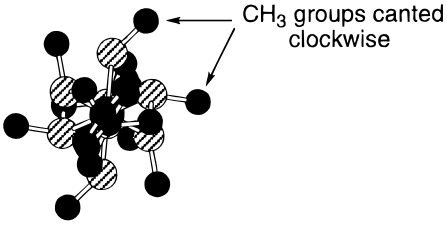

Figure 5. View of $[PhTt]_2Ni$ along the B−Ni−B vector showing the canting of the S−CH_3 groups in the same direction.

spectroscopic and structural properties consistent with a moderately strong ligand field. In this context, the new ligands complement the versatile face-capping, tridentate donors tacn, ttcn, and $HB(pz)_3^-$ by providing a S_3^- donor set. Importantly, the inherent synthetic flexibility of these borates promises a wider scope of coordination chemistry than is accessible to ttcn. Experiments in this context are directed toward (i) modifying the ligands to provide more sterically demanding substituents on sulfur and (ii) preparing bidentate derivatives, $Ph_2B(CH_2SCH_3)_2^-$.[15]

Acknowledgment. We gratefully acknowledge the financial support of the Exxon Educational Fund and DuPont Central Research and Development. C.G.R. thanks the NSF for a National Young Investigator Award (1994−9).

Supporting Information Available: Tables giving structure determination summaries, atomic coordinates, bond lengths, bond angles, anisotropic thermal parameters, and hydrogen atom parameters for $[PhTt]_2Fe$, $[RTt]_2Co$, $[PhTt]_2Co$, $[RTt]_2Ni$, and $[PhTt]_2Ni$ (27 pages). Ordering information is given on any current masthead page.

IC9511377

(15) Ge, P.; Riordan, C. G.; Yap, G. A. P.; Rheingold, A. L. Unpublished results.